

Photoluminescence Studies of Phenanthrene–Azomethyne Conjugated–Nonconjugated Multiblock Copolymer

Angelita M. Machado,^{†,‡} Marilda Munaro,[‡] Tatiana D. Martins,[§] Liliana Y. A. Dávila,[‡] Ronaldo Giro,[‡] Marília J. Caldas,[‡] Teresa D. Z. Atvars,[§] and Leni C. Akcelrud^{*,†}

Departamento de Química, Universidade Federal do Paraná, Centro Politécnico, Caixa Postal 19081, 81531-990 Curitiba, PR, Brazil; Instituto Tecnológico para o Desenvolvimento LACTEC, Centro Politécnico, 81531-990 Curitiba, PR, Brazil; Instituto de Química, Unicamp, Caixa Postal 6154, 13084-971 Campinas, SP, Brazil; and Instituto de Física, USP, Cidade Universitária, 05508-900 São Paulo, SP, Brazil

Received October 27, 2005; Revised Manuscript Received February 1, 2006

ABSTRACT: A Schiff base type polymer containing phenanthrene and an aliphatic spacer in the main chain was prepared, and its photophysical behavior in diluted and concentrated solutions as well as in film form was studied by steady-state fluorescence spectroscopy. These data indicated that ground-state fluorescent phenanthrene aggregates were present in the films. Time-resolved measurements in diluted conditions showed biexponential decay implying in different microenvironments around the chromophore. Theoretical simulations predicted aggregation in π -stack arrangement, and calculation of optical properties for small aggregates shows the introduction of new states at lower energies, in good agreement with the experimental results. Theoretical studies also forecast the possibility of domains with highly ordered morphology, which was confirmed by DSC measurements providing further support for the presence of the emitting aggregated form.

1. Introduction

The photophysics of phenanthrene and its derivatives has been explored for many years, and it is fair to say that all the important issues related to the subject have been clarified.^{1–3} However, the information about the photophysical behavior of phenanthrene when linked to a polymer chain either in a lateral chain or placed along the backbone is rather scarce. This is probably due to complexities introduced by the synergic effects involving electronic states of phenanthryl groups and the polymer chains combined with other types of interactions, such as the chemical nature and polarity of the surroundings around the fluorophore, and the conformational order of the main chain which may interfere with the Franck–Condon transitions. As a result, the emissive properties of the chromophore are greatly dependent not only on its intrinsic properties but also on the properties of the cavity where it is located.⁴ The role of the local concentration can also be important, even in cases where the total amount of the lumophore is low, due to microphase separation processes. In fact, there are several examples showing that the spectral characteristics of a polymer-bound chromophore can change dramatically in relation to the “free” molecule,⁵ as in the case of the blue light emitted from naphthalene containing poly(urethane–urea)s,⁶ stable stilbene ground-state dimers in polymers bearing this chromophore as a pendant group,⁷ and green electroluminescence from specific compositions of poly(methyl methacrylate-*co*-9-methylanthryl methacrylate).⁴ Furthermore, aggregation and several types of energy-transfer processes have been observed in intrinsically luminescent polymers in concentrated solution or in the solid state.

Aggregation in solid-state polymers can usually be detected by the pronounced changes of the spectra in either absorption, emission, or both.^{4,6,8–14} In particular, aggregation of phenan-

threne groups attached to polymer chains has already been described. In such studies, phenanthrene is randomly attached as a pendant group, and the aggregation has been explained in terms of a process induced by the polarity of the group to which it is linked and not by the chromophore itself.²

In the present contribution we study a phenanthrene-containing conjugated–nonconjugated block copolymer, beginning from the synthesis and proceeding through photophysical and thermal characterization, theoretical modeling, and calculation of optical properties for different aggregated systems. We expect to add more insight into the photophysical behavior of phenanthrene-containing polymers, since this is the first work in which the lumophore is located in the backbone in a controlled configuration, making it possible to observe the effects of the anchoring to a polymer chain as compared to the “free” chromophore.

The strategy explored the concept of multiblock conjugated–nonconjugated copolymers^{15,16} where the emitting block 1,4-phenylenemethylidene nitrile–9,10-phenanthrylenenitrile-methylidene was interspersed with octamethylene segments, as shown in Figure 1a. The main-chain aliphatic spacer has a double function: to improve solubility and act as a nonconjugated barrier that isolates the emissive center, providing control of the size of the emissive center.

The configuration with phenanthrene placed along the polymer backbone as a constituent of the structural unit imparts some structural hindrance to same-chain lumophore interactions, and possibly the only phenanthrene associations will be among the interchain species, making it possible to probe interchain interactions by the spectroscopic behavior of the system.

2. Experimental Section

2.1. Materials. *N*-Methylpyrrolidone (NMP) (Vetec, Brazil) and dimethylformamide (DMF) (Vetec, Brazil) were distilled under reduced pressure (10 and 5 mmHg, respectively) and stored under molecular sieves (4 Å). Seringaldehyde, 1,8-dibromooctane, anhydrous potassium carbonate (Vetec), poly(phosphoric acid) (Vetec),

[†] Universidade Federal do Paraná.

[‡] Instituto Tecnológico para o Desenvolvimento LACTEC.

[§] Instituto de Química.

[‡] Cidade Universitária.

* Corresponding author. E-mail: leniak10@yahoo.com.br.com.br.

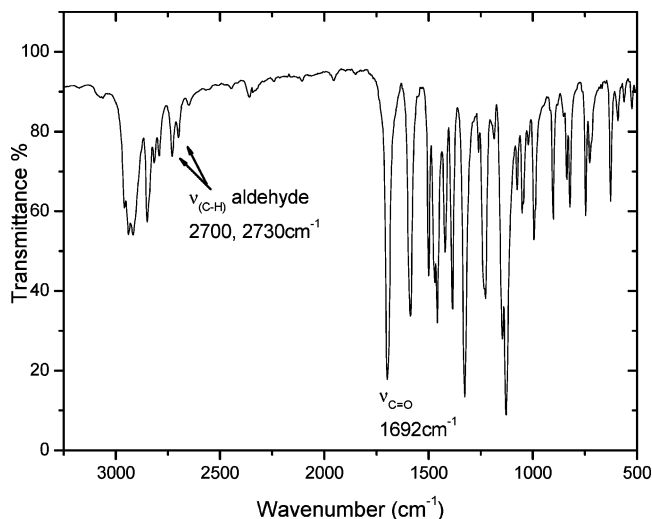


Figure 1. FT-IR spectrum of 1,2-bis(4-formyl-2,6-dimethoxy)octane (KBr disk).

lithium chloride, toluenesulfonic acid (Vetec), and 9,10-diaminophenanthrene were purchased from Sigma-Aldrich Chemical Co. and were used without further treatment.

2.2. Monomer Synthesis and Polymerization Procedure. *1,2-Bis(4-formyl-2,6-dimethoxy)octane.* A mixture of 10 g of 3,5-dimethoxy-4-hydroxybenzaldehyde (0.055 mol) and 5.06 mL of 1,8-dibromooctane (0.028 mol) was dissolved in 140 mL of DMF under nitrogen. The temperature was raised to 60 °C, and after the addition of calcium carbonate the mixture was refluxed for 24 h, cooled to room temperature, and poured over 2 L of water. The solid was separated and washed with 300 mL of ethanol/water (5:1).

Poly[oxyoctyleneoxy-(2,6-dimethoxy-1,4-phenylenemethylideneimide)-9,10-phenanthrylenenitrilomethylidene]. A mixture of 32 mg (0.14 mmol) of 9,10-diaminophenanthrene, 0.3 mL of poly(phosphoric acid), 50 mg of phosphorus pentoxide, 50 mg of toluenesulfonic acid, and 10 mL of NMP was refluxed under nitrogen for 30 min. After that, 68 mg (0.14 mmol) of 1,2-bis(4-formyl-2,6-dimethoxy)octane was added, and the mixture was kept at 110 °C for 96 h under stirring and subsequently poured over 2 L of a saturated aqueous solution of potassium carbonate and stirred for 1 h. The final material was filtered, washed with water, and dried under vacuum.

2.3. Equipment. A Waters gel permeation chromatograph equipped with two columns HR4E and HR5E (polystyrene), pump model 1500, was used for the molecular weight determination. The solvent was DMF, in a flux of 0.6 mL min⁻¹ at 45 °C, and the columns were connected to a dual detector (UV, refraction index). The calibration was based on PS standards.

The monomers and the polymer were characterized by FTIR and NMR spectrometry, and the data are compared with the literature. Samples for FTIR measurements were prepared as KBr disks. Spectra were taken in a Bomem MB 100 FTIR spectrophotometer, in the spectral range of 600–4000 cm⁻¹, with resolution of 2 cm⁻¹, and 16 scans.

A NMR Brücker 400 MHz Advance series with ¹³C at 100 MHz and ¹H at 400 MHz equipment or an ac 200 MHz Brücker with ¹³C at 50 MHz and ¹H at 200 MHz was used. All NMR experiments used CDCl₃ as a solvent and TMS as internal standard.

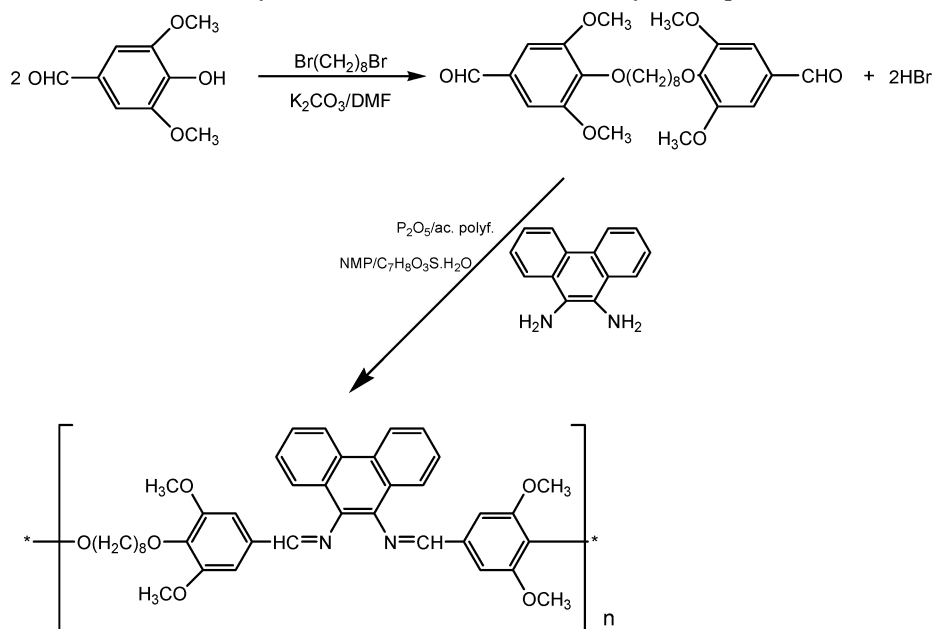
A 204 F1 Netzsch equipment was used for the DSC measurements. Typically the sample was heated from room temperature to 50 °C and quenched to -100 °C. It was then heated to 50 °C, at a rate of 10 °C/min, under nitrogen flux (15 mL/min). The same procedure was repeated with the same samples annealed for 24 h at 25 °C. Only the heating parts of the cycle were registered.

A spectrophotometer UV–vis Shimadzu model NIR 3101 was used for the electronic absorption spectra.

Steady-state fluorescence spectra were recorded using a ISS-PC1 spectrofluorimeter operating with a 300 W Xe arc lamp. Solutions of the copolymer in NMP were prepared with three concentrations in terms of moles of phenanthrene (10⁻⁵, 10⁻⁴, and 10⁻³ mol L⁻¹). A triangular quartz cuvette was employed to reduce the inner filter effect when spectrum of the higher concentrate solutions was recorded. Emission spectrum was recorded from 325 to 700 nm, with excitation depending on the concentration of the solutions: λ_{exc} = 310 nm for 10⁻⁵ mol L⁻¹ and 10⁻⁴ mol L⁻¹; λ_{exc} = 423 nm for 10⁻³ mol L⁻¹. We also recorded excitation spectra for all samples using λ_{em} = 360 and 530 nm. For the copolymer films, we recorded the emission spectra from 400 to 600 nm using λ_{exc} = 370 nm and the excitation spectra from 300 to 500 nm using λ_{em} = 495 nm. The quantum yield of the copolymer emission in solution was also determined by the steady-state fluorescence using 9,10-diphenylanthracene as standard.^{17,18}

Dynamic fluorescence decay was performed at room temperature by single photon counting (Edinburgh Analytical nF900 system)

Scheme 1. Synthetic Routes for Monomer and Polymer Preparation



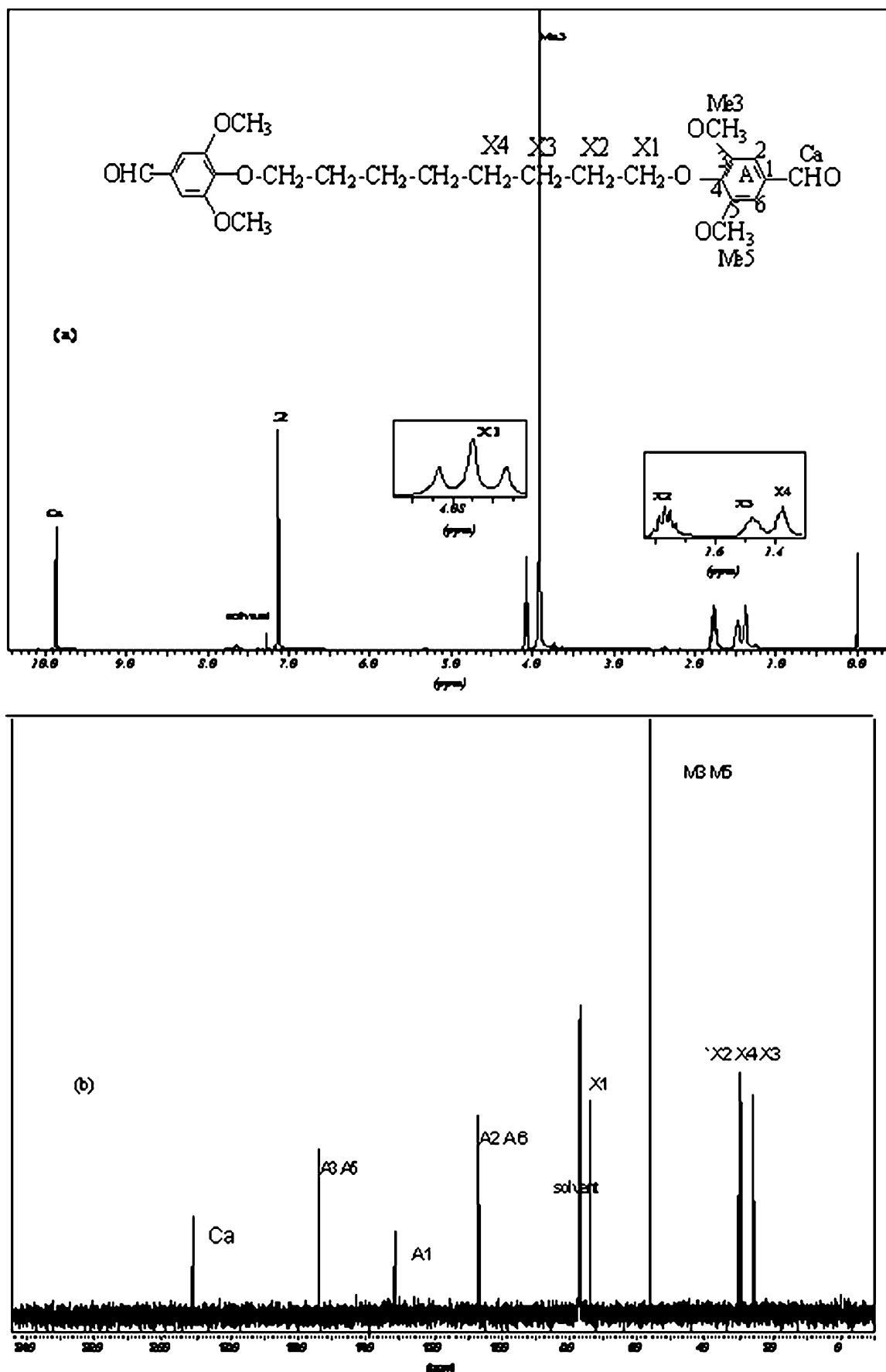


Figure 2. (a) ^1H NMR and (b) ^{13}C NMR spectra of 1,2-bis(4-formyl-2,6-dimethoxy)octane (CDCl_3).

operating with a pulsed hydrogen lamp at a repetition rate of 40 kHz. The excitation wavelength was coincident with the excitation peak $\lambda_{\text{exc}} = 310$ nm for the chromophoric absorption, and the

emission was collected in the fluorescence maximum $\lambda_{\text{em}} = 356$ nm. The sample solutions and the copolymer films were degassed and maintained in a sealed quartz tube. The instrument response

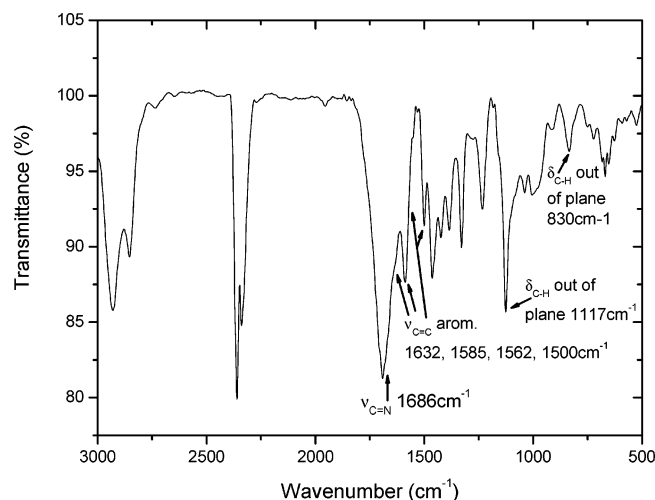


Figure 3. FT-IR spectrum of poly[oxyoctyleneoxy-(2,6-dimethoxy-1,4-phenylenemethylidinedinitrile)-9,10-phenanthrylenenitrilomethylidene] (KBr disk).

was determined at every measurement using Ludox as scatterer. At least 10^4 counts were collected in the peak channel. Deconvolution of the lamp pulse was performed by nonlinear least-squares routines using the software supplied by Edinburg. The best fit was achieved when the χ^2 is close to one, and the residual distribution was random.

3. Computational Methods

Theoretical simulations were done using a multiscale strategy: to study long chains and aggregation properties for these copolymers, we used classical molecular mechanics (MM), and the study was refined for specific small oligomers using quantum mechanical calculations with AM1.¹⁹ Optical properties were calculated for special configurations with INDO/SCI.^{20,21} For linear chains we always end the oligomer on both sides by half the nonconjugated segment. We have designated these copolymer chains as σ -oligomers, since the chromophores are linked to each other through the σ bonds of the alkyl spacer.

The conformational search for the supramolecular aggregates was performed with the empirical force field UNIVERSAL 1.02 (UFF) as implemented in the Cerius2 software package.²² The UFF terms include van der Waals and electrostatic interactions for nonbonded atoms, critical for investigations of the supramolecular packing. In all MM geometrical optimizations, the following convergence criteria was used: maximum force of 0.005 kcal/(mol Å), root-mean-square (rms) deviations of 0.001 kcal/(mol Å), energy differences of 0.0001 kcal/mol, maximum atomic displacement of 0.0005 Å, and rms gradient of 0.000 01 Å.

4. Results and Discussion

4.1. Synthesis and Structural Characterization. The synthetic route to the polymer is depicted in Scheme 1. The chemical structure of the monomer 1,2-bis(4-formyl-2,6-dimethoxy)octane and of poly[oxyoctyleneoxy-(2,6-dimethoxy-1,4-phenylenemethylidinedinitrile)-9,10-phenanthrylenenitrilomethylidene] was confirmed by FTIR and ^1H NMR and ^{13}C NMR spectra, shown in Figures 1–4. The apparent molecular weight of the copolymer was determined by GPC as $\bar{M}_n = 13\,000$, $\bar{M}_w = 15\,600\text{ g mol}^{-1}$, and polydispersity index = 1.2. No byproducts were detected.

The optimized geometry obtained through AM1 calculations shows the phenanthryl groups in a planar configuration, practically orthogonal to the main chain, with the phenyl groups

distorted from the phenanthrene planes as shown in Figure 5b. Therefore, as expected, the monomeric unit (phenylazo-methyne–phenanthrene) is not conjugated, and the emission center is confined to the phenanthrene moiety, with the sequences of methylene inert spacers conferring some flexibility to the main chain.

The DSC thermograms of the poly(azomethyne) are shown in Figure 6. The most relevant findings were a change in slope of the baseline attributed to a glass transition around $-53\text{ }^\circ\text{C}$, an endotherm attributed to the melting of a crystalline phase at $18.5\text{ }^\circ\text{C}$, and another transition at $-3\text{ }^\circ\text{C}$. The curvatures seen at the very beginning of the scans at the low-temperature side are artifacts commonly seen in DSC runs and are meaningless. Both glass transition and melting were very reproducible, no matter how many runs were performed with the same sample. The transition at $-3\text{ }^\circ\text{C}$, tentatively attributed to crystallization, however, was only seen if after the first run the samples were annealed at $25\text{ }^\circ\text{C}$ during some time, typically 24 h. This indicates that the rearrangement of the chains after melting required some time to achieve completion, and a definitive assignment of the transition would require more work on this specific point. At this stage one should ask what is really melting, since the material is a multiblock copolymer with chemically distinct segments linked along the backbone. Previous works have demonstrated that similar multiblock copolymers, differing only in the hard (chromophoric) blocks which were connected to the same octamethylene flexible spacers were in fact phase-separated materials. These findings were based on the selective plasticization of the spacer phase,²³ and it was also concluded that the requirement for phase separation in some kinds of copolymers is not necessarily long block length but rather flexible chain containing two highly dissimilar segments. The theoretical data seem to indicate that the melting is occurring in the hard blocks, since the tendency to π -stacking is very high and favored by the chain configuration. Linear copolyesters containing phenanthrene and naphthalene also have shown a certain degree of crystallinity, which increased with the phenanthrene content in the chains.²⁴

4.2. Photophysical Behavior. The photophysical study was performed in NMP solutions in concentrations of 10^{-3} , 10^{-4} , and 10^{-5} M . Figure 7 displays fluorescence emission and excitation spectra. When compared to the spectrum of phenanthrene itself, the emission spectra of the polymer have shown two distinct features: the first is the red shift in relation to phenanthrene in *n*-hexane diluted solutions.¹ This spectral shift is usually found for aromatic compounds linked to polymeric chains or containing aliphatic substituents^{25–29} although here we must also consider that the conjugation with the azomethyne bridge is a source of electronic interaction which might lead to additional band shift. The second feature is related to the peak broadening and less resolved vibronic structure, as compared to the electronic absorption and emission spectra of phenanthrene itself.³⁰ This effect has also been observed for various aromatic hydrocarbons linked to polymeric chains and has been interpreted in terms of the conformational disorder of the main chain, leading to an inhomogeneous band broadening.^{4,27–29}

The quantum yield determined from the steady-state fluorescence emission of this copolymer was $\varphi_f = 0.22$. This value is higher than that of phenanthrene itself, ca. $\varphi_f = 0.13$, and is similar to others found for some phenanthrene derivatives.^{26,31,32}

Going from the more diluted to the more concentrated solutions a slight broadening was detected, with a shoulder at

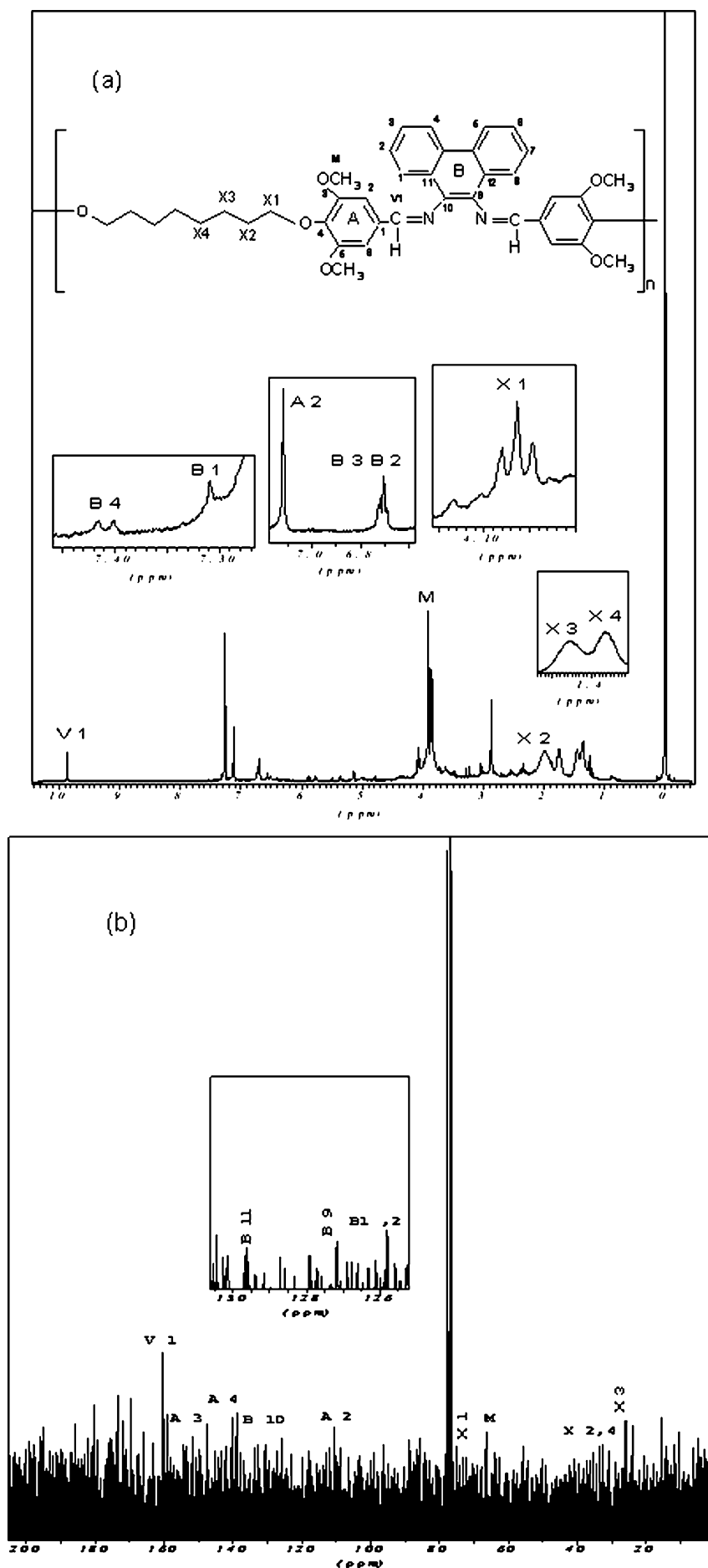


Figure 4. (a) ^1H NMR and (b) ^{13}C NMR spectra of polymer taken in CDCl_3 and their assignment.

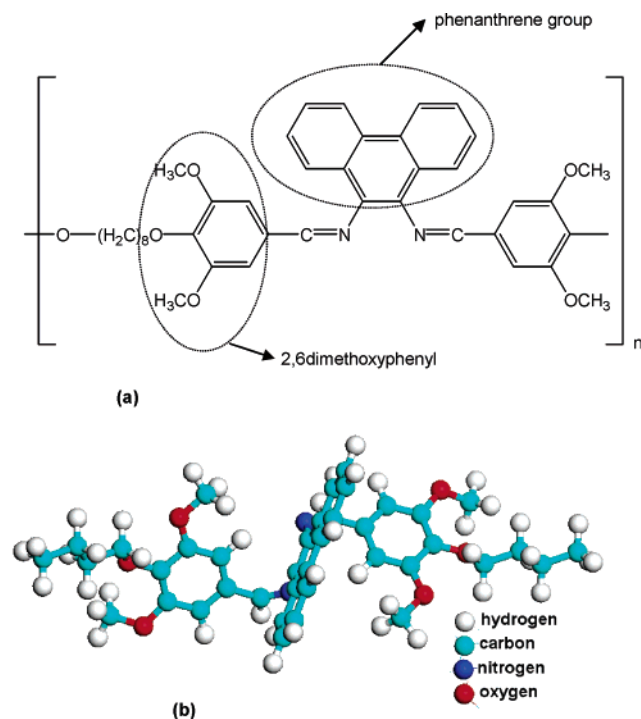


Figure 5. (a) Chemical structure of the multiblock conjugated–nonconjugated poly[oxyoctyleneoxy-(2,6-dimethoxy-1,4-phenylenemethyldinitrile-9,10-phenanthrylenenitrilomethylidene)] and (b) computer-optimized configuration of one structural unit.

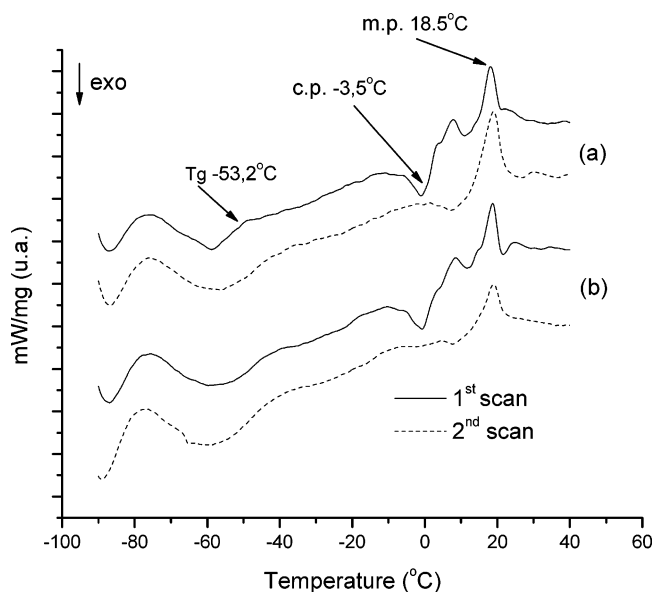


Figure 6. DSC thermogram of the copolymer showing glass transition, crystallization, and melting peaks: (a) first and second scans were run in sequence; (b) second scan run after 24 h annealing at 25 °C.

410 nm in the emission spectra of solution 10^{-5} M in relation to the 10^{-4} M, but the main emission peaked at 359 nm for both. The most striking result, however, was the dramatic redshifting of the 10^{-3} M solution with respect to the more diluted ones. Two main peaks were registered at 496 and 533 nm (Figure 7c). Monitoring the two more diluted solutions (10^{-5} and 10^{-4} M) at 366 nm, it was observed that the excitation spectra peaked at 370 nm, whereas the excitation in the red region brought about a weak emission from the concentrated solution also very red-shifted in relation to that of the diluted solutions. Although red-shifted, the emission spectrum of the higher concentrate solution was a mirror image of the excita-

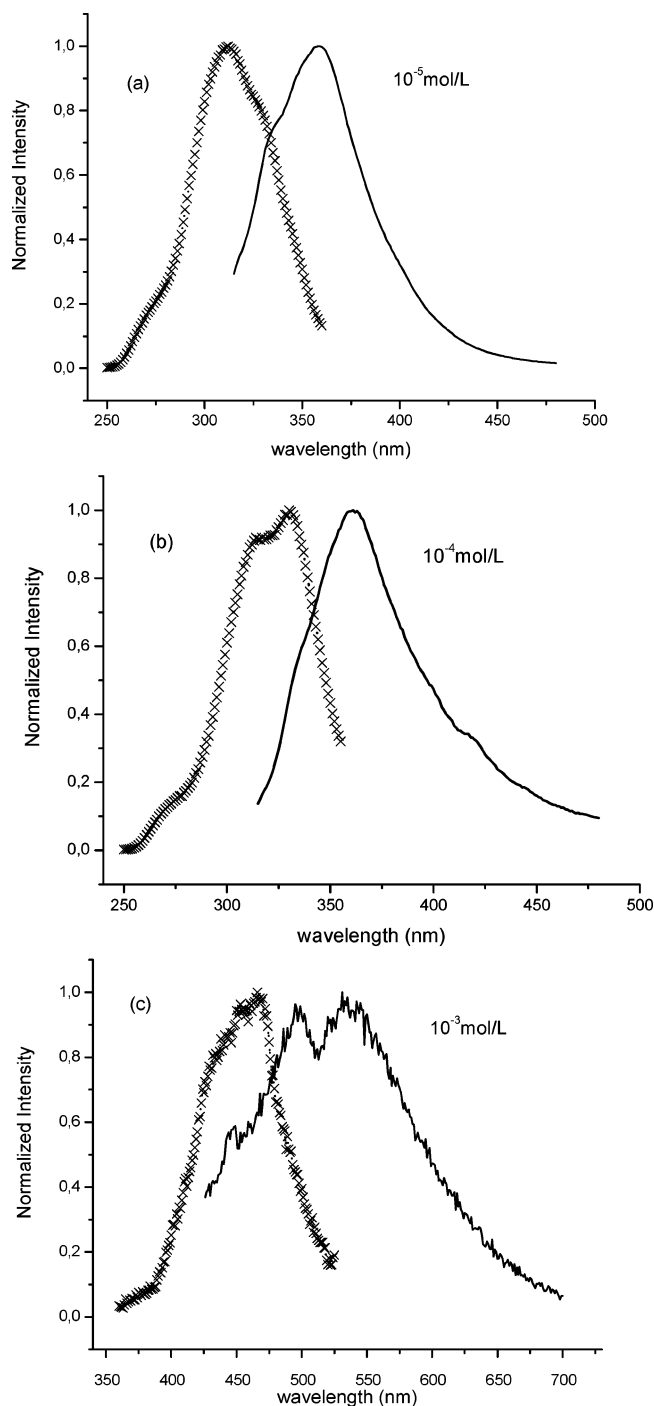


Figure 7. Fluorescence (—) and excitation (×) spectra of the copolymer in NMP solutions: (a) $\lambda_{\text{exc}} = 334$ nm, $\lambda_{\text{em}} = 366$ nm, 10^{-5} M; (b) $\lambda_{\text{exc}} = 311$ nm, $\lambda_{\text{em}} = 360$ nm, 10^{-4} M; (c) $\lambda_{\text{exc}} = 423$ nm, $\lambda_{\text{em}} = 531$ nm, 10^{-3} M.

tion spectra, indicating that the absorbing and emitting species were the same, probably present in the electronic ground state. Since we have used triangular cuvettes and front-face excitation and detection, we can assume that the greater spectral changes of the more concentrated solution should be other than the inner filter effect. In addition, because of the excitation and emission spectra are mirror images, we should suggest that phenanthrene moieties are partially aggregated in more concentrated solutions.

The emission ($\lambda_{\text{exc}} = 370$ nm) and excitation ($\lambda_{\text{em}} = 495$ nm) spectra of the polymer films, shown in Figure 8, add more support to that supposition, demonstrating that in films only

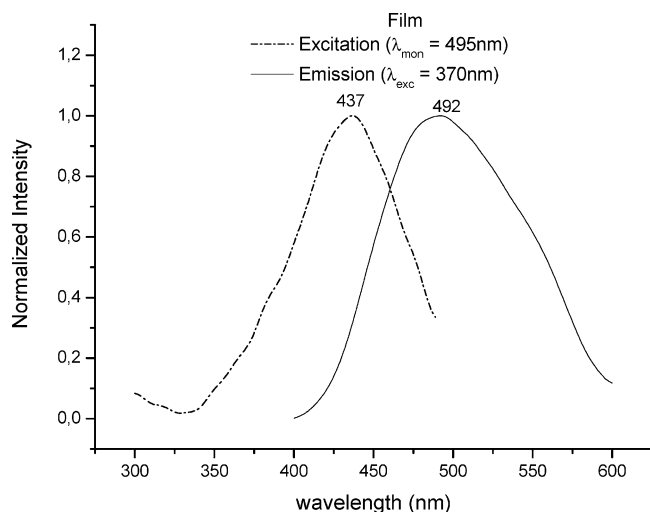


Figure 8. Emission ($\lambda_{\text{exc}} = 370$ nm) and excitation ($\lambda_{\text{em}} = 495$ nm) spectra in of the copolymer in the solid state.

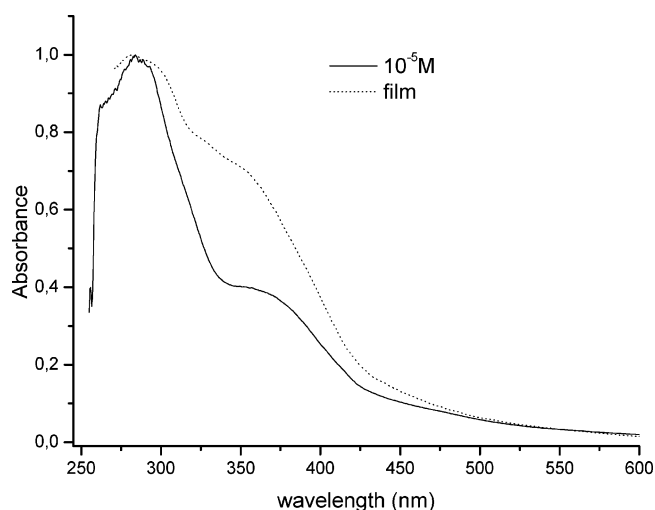


Figure 9. Electronic absorption spectra of the copolymer in solution of 10^{-5} M NMP and in film form.

the aggregates are the emitting units. Differences of the electronic absorption spectra of the diluted solution (10^{-5} M) and film shown in Figure 9 agree with the assumption of the presence of phenanthrene aggregates in the solid state, since the solid-state spectrum presented a more pronounced intensity at the red edge of the absorption band.

To interpret these findings in terms of interchromophore association, it is important to bear in mind that phenanthrene and its derivatives are a family of aromatic compounds that apart from normal fluorescence, p-type delayed fluorescence, and phosphorescence emissions^{1–23,33} does not easily form excimer species although self-quenching is observed at higher concentrated solutions.^{34–40} Excimer species were only detected in restricted media⁴¹ such as ultrathin LB films⁴² and symmetrically substituted diphenanthrylpropanes.⁴³

Concerning the polymers bearing phenanthryl groups, the reported results refer to systems where the chromophore is placed as a pendant group and not belonging to the main chain,³⁵ as in the present case. The formation of excimers has been demonstrated in many of these studies, as in poly[2-(9-phenanthrylethyl vinyl ether)] and poly(9-vinylphenanthrene)^{36,44} and poly(9-phenanthryl methacrylate), poly(2-(9-phenanthryl)-ethyl vinyl ether).⁴⁴ The intramolecular excimer interactions were considered to be the main cause of the decrease in emission

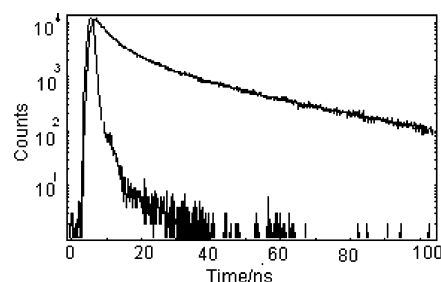


Figure 10. Fluorescence decay of the copolymer (10^{-3} M NMP). $\lambda_{\text{em}} = 356$ nm and $\lambda_{\text{exc}} = 311$ nm. This includes lamp profile and the superimposed best fit to the experimental data.

intensity. The reason is that, in general, the excimer has lower fluorescence quantum yield compared with the isolate lumophore, and consequently, the total emission intensity should also be lower.^{36,45}

Figure 10 shows the emission decay of the lamp pulse (faster decay), the experimental fluorescence decay, and the fitted decay (continuous line) superposed to the experimental data. In our case, the fluorescence decay of the copolymer in NMP solution measured with $\lambda_{\text{exc}} = 310$ nm and $\lambda_{\text{em}} = 356$ nm showed a biexponential decay with a longer lifetime of 33.9 ± 0.4 ns and a shorter one of 9.0 ± 0.2 ns, as shown in Figure 10 for the 10^{-4} M solution. We accomplished the quality of the fit by adjusting of the experimental curve using the parameter χ^2 , which is an average parameter covering the entire range of data points. The parameter obtained in our work was $\chi^2 = 1.143$ with a residual random distribution, indicating that a good deconvolution of the experimental decay curve has been achieved. As noted, for phenanthrene itself the fluorescence emission is always monoexponential and dependent on the solvent. Values of $\tau_F = 55$ ns,³¹ 57 ns,³² 57.3 ns,³⁶ 59.5 ns in *n*-heptane solution, and 63 ns in isobutyl alcohol¹ have been reported, with the corresponding quantum yields of $\phi_F = 0.13$. Our attempts to measure the decay time by excitation of the aggregated form ($\lambda_{\text{exc}} = 423$ nm) were not successful due to the large scattering coming from the 10^{-3} M NMP solution and the very low intensity of the aggregate emission. Comparing with the phenanthrene molecule, derivatives have shown shorter fluorescence lifetimes (from 20 to 45 ns) and higher quantum yields (from 0.14 to 0.3), in agreement with our results.^{24,31,32,36–47} For example, it has been reported that the lifetime of the excimer emission in poly(vinylphenanthrene) has a lifetime of 6 ns,³⁶ whereas two times (14 and 44 ns) were found for phenanthrene-labeled poly(styrene-*b*-poly(ethylene-*co*-butylene)-*b*-polystyrene).⁴⁵

The biexponential decay found for the phenanthrene moieties of the copolymer in dilute solutions and recorded at the wavelength where the isolate form is emitting implies in the existence of different environments surrounding each lumophore. These different environments surrounding each lumophore arise from distinct conformations of the aliphatic residue of the main chain leading to distinct average distances among the lumophores. Because of the possibility of those distinct conformations, some segments could assume coiled conformations while others would be more extended, depending on the solvent capability. Those phenanthrene moieties located in more coiled domains would be more protected than those located in more extended segments. When in extended conformation, they will be exposed to quenching due to several types possible of processes, including those due to residual oxygen dissolved in the solvent. This picture to explain the biexponential decay is consistent with other reported data^{4,25,27,48,49} in which the longer

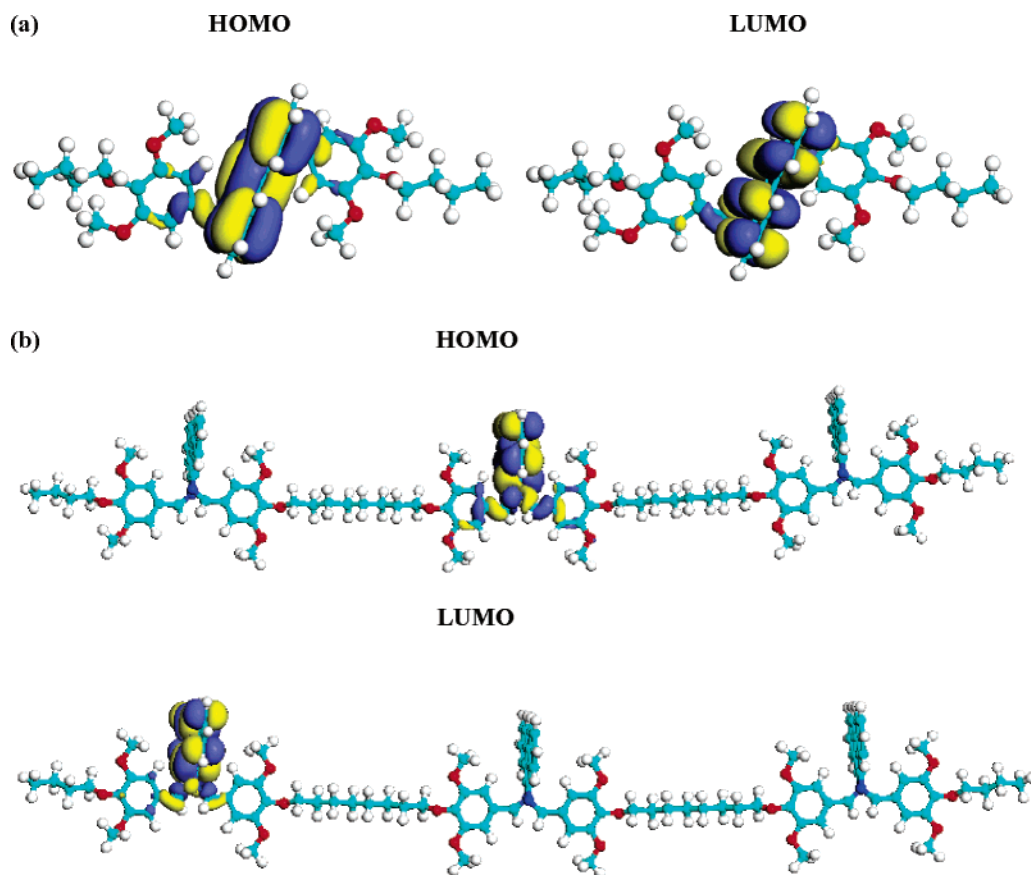


Figure 11. Delocalization pattern for the frontier molecular orbitals HOMO (highest occupied molecular orbital) and LUMO (lowest unoccupied molecular orbital) of (a) repeating unit and (b) trimer. Results from AM1 calculations. Note that the charge density is concentrated on the phenanthrene group.

lifetime is closer to that of the “free” chromophores and was due to the more protected group and the shorter to those more susceptible to quenching processes.^{1,4,27,50}

The DSC data showed that this polymer has a glass transition at $-53\text{ }^{\circ}\text{C}$ and a melting point at $18.5\text{ }^{\circ}\text{C}$. All of the photophysical properties were measured at room temperature, ca. $20\text{ }^{\circ}\text{C}$, therefore above the glass transition temperature and around the melting point. In previous works using several polymers and copolymers, some of us showed the strong effect of the phase transition on the photoluminescence properties of the materials.^{28,29,51} In particular, we have demonstrated that above the glass transition temperature part of the interchain species can dissociate⁵¹ with the corresponding decrease of interchain emission. This should be one of the reasons for the lower intensity emission of phenanthrene aggregates: there is a small population of such species in addition to the usual lower fluorescence quantum yield of the aromatic molecules.^{1,50} Nevertheless, since we are working near the melting point, aggregates are still present since the small crystals behave as cross-links for macromolecular segments belonging to the viscous liquid phase at temperature above the T_g . Thus, the interchromophoric emission in the present case is still possible due to the presence of residual ordered segments. The temperature effect on the photophysical properties of this material is in progress.

4.3. Theoretical Simulations of Aggregate Structures and Optical Properties. To gain deeper insight for the processes occurring in the material, we tried to map the possible aggregate structures and their corresponding optical properties. We first optimized the structure of an isolated chain composed by one

to three repetitive units and then simulated the effect of packing or assembling several long chains. The optimized geometry obtained through AM1 for the trimer resulted in a linear backbone with the phenanthrene groups arranged perpendicularly to the chain direction. Analysis of the frontier molecular orbitals HOMO (highest occupied molecular orbital) and LUMO (lowest unoccupied molecular orbital) for the isolate chain trimer shows that both are localized almost exclusively over the phenanthrene group (Figure 11), with some spreading over the imine segments. In agreement with the experimental spectrum in solution the ZINDO/S-CI simulated absorption spectrum shows the absorption threshold about 340 nm ($\sim 3.6\text{ eV}$), indicating that the $\pi-\pi^*$ transition is confined to the single phenanthrene units.

Once the geometry for these σ -oligomers was obtained, we proceeded to study the supramolecular arrangement with molecular mechanics. We analyzed various possible aggregate units beginning with the coupling of two trimers. It is interesting to note in the final structure that 2,6 dimethoxyphenylene (MeP) rings from adjacent chains couple in pairs in a π -stack fashion with an interplanar distance between MePs on neighbor chains of 3.45 \AA . This distance is similar to those usually observed for dimers and excimers of aromatic molecules in solid state.^{37,38} We also calculated with ZINDO/SCI the optical absorption for the π -aggregates which can be compared with the experimental absorption spectrum for the higher concentrated solution by weighting mixture of isolated copolymers and packed structures (Figure 12). In the experimental curve we find a high-energy peak at $\sim 310\text{ nm}$, with a pronounced shoulder to lower energies with the optical threshold at 368 nm . We can see a very good

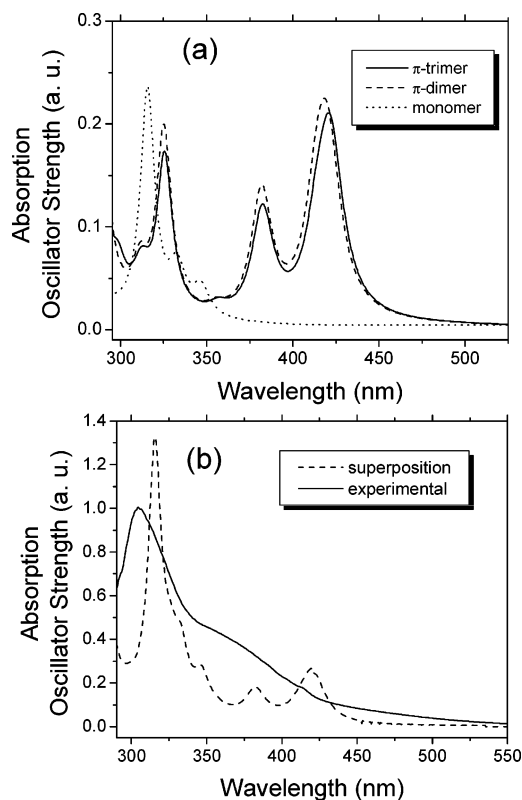


Figure 12. Electronic properties for π -aggregates: (a) simulated absorption spectra for the π -dimer and π -trimer, obtained from ZINDO/S-CI calculations for the UFF geometries (we include the absorption for the monomer for comparison); (b) experimental absorption spectrum of LaPPS19 10^{-4} M in NMP compared to a simulation of the absorption spectrum for π -aggregates embedded in isolated π -oligomers environment (here we used $\gg 18\%$ of aggregated emitting centers).

agreement between the curves, and indeed our value for the main absorption peak for the isolated oligomer (Figure 12a) is almost exactly coincident with the main experimental absorption, at ~ 316 nm, as is the optical threshold for the mixture.

5. Conclusions

The conjugated–nonconjugated multiblock copolymer poly-[oxyoctyleneoxy-(2,6-dimethoxy-1,4-phenylenemethylidene)trile-9,10-phenanthrylenenitrilomethylidene] has been prepared from the condensation of 1,2-bis(4-formyl-2,6-dimethoxy)octane with 9,10-diaminophenanthrene. This copolymer contains a phenanthrene group inserted along the polymer backbone through azomethyne bridges, separated by aliphatic groups that enhanced the polymer solubility. Comparing with the phenanthrene molecule, the copolymer emission in solution has a higher quantum yield and longer lifetime. The photophysical behavior of the polymer in concentrated solution and film, compared to that of diluted solutions, indicated the presence electronic of ground-state phenanthrene aggregates whose emission is red-shifted compared to the isolated chromophore. Theoretical simulations of the optical properties for the isolated copolymer confirmed that the emissive state is localized over the phenanthrene moieties; furthermore, absorption/emission spectra for π -stacked aggregates resulted strikingly red-shifted compared to the isolated forms, as seen experimentally.

Acknowledgment. The authors thank CNPq and MCT/PADCT/IMMMP for financial support. Also, T.D.Z.A., T.D.M., R.G., and M.J.C. thank FAPESP; T.D.Z.A. and T.D.M. thank

FAPESP/Unicamp; and L.A. and A.M.M. thank LACTEC.

References and Notes

- (1) Birks, J. B. *Photophysics of Aromatic Molecules*; Wiley-Interscience: London, 1970.
- (2) Ni, S.; Zhang, P.; Wang, Y.; Winnik, M. A. *Macromolecules* **1994**, *27*, 5742.
- (3) Ng, D.; Guillet, J. E. *Macromolecules* **1982**, *15*, 728.
- (4) Deus, J. F.; Andrade, M. L.; Atvars, T. D. Z.; Akcelrud, L. *Chem. Phys.* **2004**, *297*, 177.
- (5) Akcelrud, L. *Prog. Polym. Sci.* **2003**, *28/6*, 875.
- (6) Simas, E. R.; Akcelrud, L. *J. Lumin.* **2003**, *105*, 69.
- (7) Aguiar, M.; Hu, B.; Karasz, F. E.; Akcelrud, L. *Macromolecules* **1996**, *29*, 3161.
- (8) Machado, A. M.; Motta Neto, J. D.; Cossello, R. F.; Atvars, T. D. Z.; Ding, L.; Karasz, F. E.; Akcelrud, L. *Polymer* **2005**, *46/8*, 2452.
- (9) Woo, H. S.; Lhost, O.; Graham, S. C.; Brédas, J. L.; Schenk, R.; Mullen, K. *Synth. Met.* **1993**, *59*, 13.
- (10) Tian, B.; Zerbi, G.; Schenk, R.; Mullen, K. J. *Chem. Phys.* **1991**, *95*, 3191.
- (11) Ohnishi, T.; Doi, S.; Tsuchida, Y.; Noguchi, T. *IEEE Trans. Electron. Dev.* **1997**, *44*, 1253.
- (12) Von Seggern, H.; Wnkelp, P. S.; Zhang, C.; Schimdt, H. W. *Macromol. J. Chem. Phys.* **1994**, *195*, 2023.
- (13) Zheng, S.; Shi, J.; Mateu, R. *Chem. Mater.* **2000**, *12*, 1814.
- (14) Burn, P. L.; Holmes, A. B.; Kraft, A.; Bradley, D. D. C.; Brown, A. R.; Friend, R. H.; Gymer, R. W. *Nature (London)* **1992**, *356/6364*, 47.
- (15) Hu, B.; Yang, Z.; Karasz, F. E. *J. Appl. Phys.* **1994**, *76/4*, 2419.
- (16) Pinto, M. R.; Hu, B.; Karasz, F. E.; Akcelrud, L. *Polymer* **2000**, *41*, 2603.
- (17) Melhuish, W. H. *Quantum Efficiencies of Fluorescence of Organic Substances* **1961**, *65*, 229.
- (18) Rusakowicz, R.; Testa, A. C. J. *Phys. Chem.* **1968**, *72*, 2680.
- (19) Dewar, M. J. S.; Zoebish, E. G.; Healy, E. F.; Stewart, J. J. P. *J. Am. Chem. Soc.* **1985**, *107*, 3902.
- (20) Ridley, J.; Zerner, M. C. *Theor. Chim. Acta* **1976**, *42*, 223. Edwards, W. D.; Zerner, M. C. *Theor. Chim. Acta* **1987**, *72*, 347.
- (21) Bolívar-Marinez, L. E.; Galvão, D. S.; Caldas, M. J. J. *Phys. Chem. B* **1999**, *103*, 2993.
- (22) Rappé, A. K.; Casewit, C. J.; Goddard, W. A., III; Skiff, W. M. J. *Am. Chem. Soc.* **1992**, *114*, 10024.
- (23) Gurel, E. E.; Pasco, S. T.; Karasz, F. E. *Polymer* **2000**, *41*, 6969.
- (24) Yonetake, K.; Yashiro, H.; Madachi, N.; Ueda, M.; Masuko, T. *Polymer* **1998**, *39*, 5523.
- (25) Kamat, P. V. *Anal. Chem.* **1987**, *59/21*, 1636.
- (26) Atvars, T. D. Z.; Dorado, A. C.; Pierola, I. F. *Polym. Networks Blends* **1997**, *7*, 111.
- (27) Andrade, M. L.; Atvars, T. D. Z. *J. Phys. Chem. B* **2004**, *108*, 3975.
- (28) Schurr, O.; Yamaki, S. B.; Wang, C.; Atvars, T. D. Z.; Weiss, R. G. *Macromolecules* **2003**, *36*, 3485.
- (29) Luo, C.; Atvars, T. D. Z.; Meakin, P.; Hill, A. J.; Weiss, R. G. *J. Am. Chem. Soc.* **2003**, *125*, 11879.
- (30) Martins, T. D. Dissertation, Unicamp (Brazil), 2001.
- (31) Berlman, I. B. *Handbook of Fluorescence Spectra of Aromatic Molecules*, 2nd ed.; Academic Press: New York, 1971.
- (32) Lewis, F. D.; Baranczyk, S. V.; Burch, E. L. *J. Am. Chem. Soc.* **1991**, *114*, 3866.
- (33) Parker, C. A. *Photoluminescence of Solutions*; Elsevier: Amsterdam, 1968.
- (34) Turro, N. J.; Hammond, W. B. National Science Foundation Predoctoral Fellow 1964:3259.
- (35) Itoh, Y.; Webber, S. E. *Macromolecules* **1989**, *22*, 2766.
- (36) Tamal, N.; Masuhara, H.; Mataga, N. *J. Phys. Chem.* **1983**, *87*, 4461.
- (37) Birks, J. B.; Srinivasan, B. N.; McGlynn, S. P. *J. Mol. Spectrosc.* **1968**, *27*, 266.
- (38) Birks, J. B. *Rep. Prog. Phys.* **1975**, *38*, 903.
- (39) Steven, B. *Adv. Photochem.* **1971**, *8*, 161.
- (40) Sadygov, R. G.; Lim, E. C. *Chem. Phys. Lett.* **1994**, *335*, 441.
- (41) Sclavons, M.; Carlier, V.; Roover, B. D. E.; Franquinet, P.; Devaux, J.; Legras, R. *J. Appl. Polym. Sci.* **1996**, *62*, 1205.
- (42) Dutta, A. K. *Solid State Commun.* **1996**, *97*, 785.
- (43) Zachariasen, K. A.; Busse, R.; Schrader, U.; Kühnle, W. *Chem. Phys. Lett.* **1982**, *89*, 303.
- (44) Itaya, A.; Okamoto, K.; Kusabayashi, S. *Bull. Chem. Soc. Jpn.* **1977**, *50*, 52.
- (45) Liu, R.; Farinha, J. P. S.; Winnik, M. A. *Macromolecules* **1999**, *32*, 3957.
- (46) Ng, D.; Guillet, J. E. *Macromolecules* **1982**, *15*, 724.
- (47) Ng, D.; Guillet, J. E. *Macromolecules* **1982**, *15*, 728.

- (48) Yuan, H.; Párkányi, L. C.; Guo, R. K.; Wu, F. P. J. *J. Photochem. Photobiol. A: Chem.* **1992**, 63, 45.
- (49) Zhang, G.; Thomas, J. K. *J. Phys. Chem.* **1995**, 99, 11203.
- (50) Lackowicz, J. R. *Principles of Fluorescence Spectroscopy*, 2nd ed.; Kluwer Academic Publishers: New York, 1999.
- (51) Cossello, R. F.; Kowalski, E.; Rodrigues, P. C.; Akcelrud, L.; Bloise, A. C.; deAzevedo, E. R.; Bonagamba, T. J.; Atvars, T. D. Z. *Macromolecules* **2005**, 38, 925.

MA052315A